International Journal of Theoretical Physics, Vol. 46, No. 8, August 2007 (© 2007)
DOI: 10.1007/s10773-006-9326-6

Crossings and Anticrossings of Unbound States

E. Hernández[1], A. Jáuregui,[2] and A. Mondragón[1]

Received August 20, 2006; accepted November 14, 2006
Published Online: January 19, 2007

We investigate the characteristic crossings and anticrossings of energies and widths of a doublet of resonances, observed in the vicinity of, and at a degeneracy of unbound states, when the control parameters of the system are varied. This characteristic behavior is explained in terms of the local, topological structure of the surfaces that represent the complex energy eigenvalues in parameter space in the vicinity of a degeneracy point. In the simple but illustrative case of the scattering of a beam of particles by a double barrier potential well with two regions of trapping, we solved numerically the implicit, transcendental equation that defines the eigenwave numbers of a degenerate isolated doublet of resonances as functions of the real, control parameters of the system. We found that, at a degeneracy of unbound states, the surface representing the resonance eigenwave numbers as functions of the control parameters has an algebraic branch point of rank one. Unfolding the degeneracy point, crossings and anticrossings of energies and widths are obtained as projections of sections of the eigenwave number surfaces.

KEY WORDS: multiple resonances; resonances; scattering theory; phases; geometric; dynamic or topological.

1. INTRODUCTION

In recent years there has been an increasing interest in the mixing and degeneracy of an isolated doublet of unbound states of a physical system depending on control parameters. In this paper, by means of a simple and elementary example, we will exhibit the connection existing between the rich phenomenology of crossings and anticrossings of the energies and widths of the resonances in the isolated doublet of unbound states and the singularity of the surface representing the complex resonance energy eigenvalues in parameter space.

Many years ago von Neumann and Wigner (1929) explained the now familiar phenomenon of energy level repulsion and avoided level crossings of bound states observed in many quantum systems driven by hermitian Hamiltonians depending on external parameters. Teller (1937) gave a geometric interpretation of level repulsion of bound states in terms of the shape of the surfaces representing the

[1] Instituto de Física, Universidad Nacional Autónoma de México, Apdo. Postal 20-364, 01000 México D.F., México.
[2] Departamento de Física, Universidad de Sonora, Apdo. Postal 1626, Hermosillo, Sonora, México.

energy eigenvalues as functions of the control parameters near and at a degeneracy of two bound states. He found that the two degenerate levels correspond to the two sheets of an elliptic double cone. Since then, it has been realized that accidental degeneracy and level crossings, true or avoided, are important for the understanding of a wide variety of quantum phenomena (Berry, 1985). For instance, a quantum system acquires a topological phase—the Berry phase—when transported adiabatically around a path in parameter space (Berry, 1984; Wilczek and Shapere, 1989; Markovsky and Vinisky, 1989) which includes an accidental degeneracy of bound states, sometimes called a conical or diabolical point (Alden Mead, 1992; Jackiw, 1988; Moore, 1990; Vinitski *et al*., 1990; Zwanziger *et al*., 1991).

More recently, a great deal of attention has been given to the avoided level crossing phenomena of quantum energy eigenvalues in the case of unbound states (Mondragón and Hernández, 1993). Novel effects have been found which attracted considerable theoretical (Friedrich and Wintgen, 1985; Hernández and Mondragón, 1994), and very recently, also experimental interest. von Brentano (1990, 1996) examined the crossing and anticrossing properties of the energies and widths of two unbound levels mixed by a hermitian interaction and discussed the generalization of the von Neumann-Wigner theorem from bound to unbound states (Philipp *et al*., 2000; von Brentano and Philipp, 1999). The problem of the characterization of the singularities of the energy surfaces at a degeneracy of resonances arises naturally in connection with the topological phase of unbound states which was predicted by Hernández *et al*. (1992), and Mondragón and Hernández (1996, 1998), and later by Heiss (1999), and which was recently verified in a series of beautiful experiments by the Darmstadt group of Richter (Dembowski *et al*., 2001, 2003).

Some examples of simple quantum mechanical systems with double poles in the scattering matrix have been recently described. Vanroose *et al*. (1997) examined the formation of complex double poles of the scattering matrix in a two channel model with square well potentials. Recently, Hernández *et al*. (2000) investigated a one channel model with a double δ-barrier potential and showed that a double pole of the S-matrix can be induced by tuning the parameters of the model.

Korsch and Mossman (2003) made a detailed investigation of degeneracies of resonances in a double δ well in a constant (Stark) field, and Keck *et al*. (2003) extended and generalized the discussion of the Berry phase of resonance states given in Hernández *et al*. (1992) and Mondragón and Hernández (1996, 1998) to non-hermitian Hamiltonians. Vanroose (2001) generalized the double barrier potential model to the case of finite width barriers. The general theory of multiple poles of the scattering matrix, the generalized complex energy eigenfunctions and the Jordan blocks in the complex energy representation of the resolvent operator associated with them was developed by Hernández *et al*. (2003) in the framework of the theory of the analytic properties of the radial wave function.

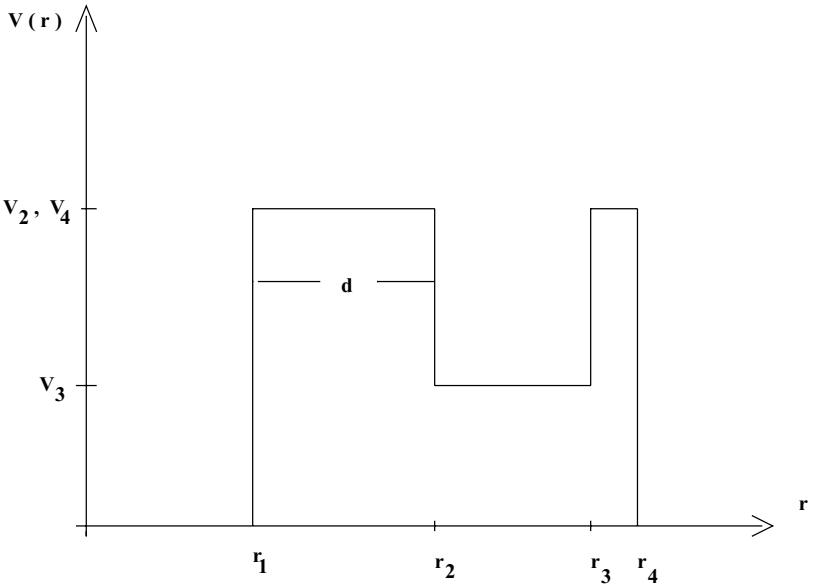

Fig. 1. The double barrier potential is such that there are two unbound states, one in each well, with equal energies and half-lives. The control parameters of the system are d and V_3.

2. SCATTERING BY A DOUBLE BARRIER POTENTIAL

Doublets of resonances and accidental degeneracies of unbound states may occur in the scattering of a beam of particles by a potential with two regions of trapping. A simple example is provided by a spherically symmetric potential $V(r)$ in which the two regions of trapping are defined by two concentric potential wells separated by two potential barriers located between the origin of coordinates and the outer region where $V = 0$. In order to make the analysis as simple and explicit as possible, we take the wells and barriers to be square as shown in Fig. 1.

In what follows, we will consider the conditions for the occurrence of a degeneracy of unbound states in this simple system and we will be interested in the geometric and topological properties of the surfaces that represent the complex energy eigenvalues as functions of the control parameters of the system in the neighborhood of and at a degeneracy of unbound states.

2.1. The Regular Solution

The s-wave radial Schrödinger equation is

$$\frac{d^2u(k,r)}{dr^2} + (k^2 - U(r))u(k,r) = 0, \tag{1}$$

the potential $U(r) = 2mV(r)/\hbar^2$ is a double barrier such that between the origin of coordinates, and the outer region, $r > r_4$, where the particles propagate freely, there are two square potential wells separated by two square potential barriers, as shown in Fig. 1. The system has seven parameters, the positions $r_i (i = 1, 2, 3, 4)$ and heights $V_i (i = 2, 3, 4)$ of the four discontinuities of the potential. In this work, we will keep the five parameters $(V_2, V_4, r_1, r_3 - r_2, r_4 - r_3)$ fixed and will vary the depth of the outer well V_3 and the thickness of the inner barrier $d = r_2 - r_1$. In the following, we will refer to the pair of parameters (d, V_3) as the control parameters of the system.

The Jost regular solution of (1) normalized to unit slope at the origin, $\phi(k, r)$, is as follows:

In the wells,

$$\phi_1(k, r) = \frac{1}{k} \sin kr, \quad 0 \le r \le r_1, \tag{2}$$

and

$$\begin{aligned} \phi_3(k, r) = \phi_2(k, r_2)[&\cos(K_3(k)(r - r_2)) \\ &+ \alpha_2(k, d) \sin(K_3(k)(r - r_2))], \quad r_2 \le r \le r_3. \end{aligned} \tag{3}$$

In the barriers,

$$\begin{aligned} \phi_i(k, r) = \phi_{i-1}(k, r_{i-1})[&\cosh(K_i(k)(r - r_{i-1})) \\ &+ \alpha_{i-1}(k, d) \sinh(K_i(k)(r - r_{i-1}))], \\ &r_{i-1} \le r \le r_i, \quad i = 2, 4, \end{aligned} \tag{4}$$

and, in the outer region,

$$\begin{aligned} \phi_5(k, r) = \phi_4(k, r_4)[&\cos k(r - r_4) \\ &+ \alpha_4(k, d) \sin k(r - r_4)], \quad r_4 \le r < \infty. \end{aligned} \tag{5}$$

In these expressions k is the wave number of the free waves and

$$K_i(k) = (U_i - k^2)^{1/2}, \quad i = 2, 4, \tag{6}$$

$$K_3(k) = (k^2 - U_3)^{1/2}. \tag{7}$$

The functions $\alpha_i(k, d)$ are the logarithmic derivatives of the regular solution at the discontinuities of the potential,

$$\alpha_i(k, d) = \frac{1}{K_{i+1}(k)} \frac{d}{dr} \ln \phi_i(k, r)|_{r=r_i}, \quad i = 1, 2, 3, 4, \tag{8}$$

with $K_5 = k$.

The logarithmic derivatives of $\phi(k, r)$ at the consecutive discontinuities r_i and r_{i+1} are related by the matching conditions at r_{i+1},

$$\alpha_1(k) = \frac{k}{K_2(k)} \cot kr_1, \tag{9}$$

$$\alpha_2(k, d) = \frac{K_2(k)}{K_3(k)} \frac{\alpha_1(k) + \tanh(K_2(k)d)}{1 + \alpha_1(k) \tanh(K_2(k)d)}, \tag{10}$$

$$\alpha_3(k; d, V_3) = \frac{K_3(k, V_3)}{K_4(k)} \frac{\alpha_2(k, d) - \tan(K_3(k)(r_3 - r_2))}{1 + \alpha_2(k, d) \tan(K_3(k)(r_3 - r_2)}, \tag{11}$$

and

$$\alpha_4(k; d, V_3) = \frac{K_4(k)}{k} \frac{\alpha_3(k; d, V_3) + \tanh(K_4(k)(r_4 - r_3))}{1 + \alpha_3(k; d, V_3) \tanh(K_4(k)(r_4 - r_3))}. \tag{12}$$

Since the first logarithmic derivative, $\alpha_1(k)$, is explicitly known, an explicit solution for $\alpha_2(k, d)$ is obtained by substitution of the expression (9) for $\alpha_1(k)$ in Eq. (10). From the knowledge of $\alpha_2(k, d)$ and Eq. (11) we solve for $\alpha_3(k; d, V_3)$ which, combined with Eq. (12) gives an explicit solution for $\alpha_4(k; d, V_3)$. Once the logarithmic derivatives α_i are explicitly known as functions of the control parameters, an explicit expression for the regular solution $\phi(k, r)$ is obtained from Eqs. (2)–(5).

The Jost function, $f(-k)$, may now be readily obtained from the regular solution in the outer region and the knowledge of $\alpha_4(k_i; d, V_3)$. When the regular solution in the outer region, given in Eq. (5), is written as a combination of an outgoing wave $\exp(ikr)$ and an incoming wave $\exp(-ikr)$

$$\begin{aligned}\phi_5(k, r) = \phi_4(k, r_4)\frac{1}{2}[&(1 - i\alpha_4(k; V_3, d)) \exp ik(r - r_4) \\ &+ (1 + i\alpha_4(k; V_3, d)) \exp -ik(r - r_4)], \quad r_4 \le r < \infty,\end{aligned} \tag{13}$$

the coefficient of the incoming wave is the Jost function. Making use of Eqs. (4), (12) and (13) we get

$$\begin{aligned}f(-k) = &\sin kr_1[\cosh(K_2(k)d) + \alpha_1(k) \sinh(K_2(k)d)] \\ &\times [\cos(K_3(k)(r_3 - r_2)) + \alpha_2(k, d) \sin(K_3(k)(r_3 - r_2))] \\ &\times \left\{ \frac{K_4}{k}[\sinh(K_4(k)(r_4 - r_3)) + \alpha_3(k; d, V_3) \cosh(K_4(k)(r_4 - r_3))] \right. \\ &- i[\cosh(K_4(k)(r_4 - r_3)) \\ &\left. + \alpha_3(k; d, V_3) \sinh(K_4(k)(r_4 - r_3))] \right\} \exp ikr_4.\end{aligned} \tag{14}$$

2.2. The Physical Solutions

The scattering wave function, $\psi(k, r)$, is the solution of Eq. (1) which vanishes at the origin and, for values of r larger than the range of the potential, it behaves as the sum of a free incoming spherical wave of unit incoming flux plus a free outgoing spherical wave,

$$\psi(k, 0) = 0, \tag{15}$$

and

$$\lim_{r\to\infty} \{\psi(k, r) - [\exp(-ikr) - S(k)\exp(ikr)]\} = 0, \tag{16}$$

the coefficient of the outgoing spherical wave is the scattering matrix $S(k)$.

Hence, the scattering wave function, $\psi(k, r)$, and the regular solution $\phi(k, r)$ are related by

$$\psi(k, r) = \frac{-2ik}{f(-k)}\phi(k, r), \tag{17}$$

and the scattering matrix is given by

$$S(k) = \frac{f^*(-k)}{f(-k)} = \exp(i2\delta(k)), \tag{18}$$

where the Jost function $f(-k)$ is given by (14).

The cross section σ_0,

$$\sigma_0 = \frac{4\pi}{k^2}\sin^2\delta(k), \tag{19}$$

is readily computed from (14) and (18).

The zeros of the Jost function give resonance poles in the scattering wave function $\psi(k, r)$, and in the matrix $S(k)$. From (1) and (2)–(5), we also verify that all roots (zeros) of the Jost function are associated with energy eigenfunctions of the radial Schrödinger equation.

Unbound state eigenfunctions also called resonant-state or Gamow eigenfunctions are the solutions of Eq. (1) that vanish at the origin,

$$u_n(k_n, 0) = 0, \tag{20}$$

and at infinity satisfy the outgoing wave boundary condition,

$$\lim_{r\to\infty}\left[\frac{1}{u_n(k_n, r)}\frac{du_n(k_n, r)}{dr} - ik_n\right] = 0, \tag{21}$$

where k_n is a zero of the Jost function,

$$f(-k_n) = 0, \tag{22}$$

with k_n located in the fourth quadrant of the complex k-plane.

Hence, the resonant-state eigenfunctions are related to the regular solution by

$$u_n(k_n, r) = N_n^{-1}\phi(k_n, r), \tag{23}$$

where N_n is a normalization constant. From (2)–(5) we verify that due to the vanishing of $f(-k_n)$, $\phi(k_n, r)$ is now proportional to the outgoing wave solution of (1), $\exp(ik_n r)$ for r larger than the range of the potential.

3. DEGENERACY OF UNBOUND STATES

A degeneracy of unbound states, that is the equality of two (or more) complex resonance energy eigenvalues of the radial Schrödinger equation, results from the exact coincidence of two (or more) simple resonance zeros of the Jost function, which merge into one double (or higher rank) zero lying in the fourth quadrant of the complex k-plane. Hence, the condition for the occurrence of a degeneracy of two unbound states at some $k = \tilde{k}$ is that both, the Jost function and its first derivative vanish at $\tilde{k}$,

$$f(-\tilde{k}) = 0, \tag{24}$$

$$\left(\frac{df(-k)}{dk}\right)_{k=\tilde{k}} = 0, \tag{25}$$

where $f(-k)$ is given in (14).

Therefore, to locate a degeneracy of unbound states, we have to solve this system of two coupled equations with two real, independent parameters, d and V_3, whose values should be adjusted to satisfy (24) and (25).

The coupled Eqs. (24) and (25) were solved numerically. The zeros of the Jost function are found by an algebraic computer package that searches for the minima of $|f(-k)|$ in the complex k-plane. Starting with the values $V_2 = V_4 = 2, r_1 = 1, r_3 - r_2 = 1, r_4 - r_3 = 0.304892$ and $d = 2$, $V_3 = 1.04$, we find the first doublet of resonances at

$$k_1 = 2.2101546 - i0.1366887 \tag{26}$$

$$k_2 = 2.2321776 - i0.0017984. \tag{27}$$

We kept the five parameters $(V_2, V_4, r_1, r_3 - r_2, r_4 - r_3)$ fixed, and we adjusted the control parameters d and V_3 until k_1 and k_2 became equal to some common value $\tilde{k}$. Then, we computed numerically $|df(-k)/dk|$ at $k = \tilde{k}$ to verify that the second equation is also satisfied to some previously prescribed accuracy. Proceeding in this way, we found that by fine tuning the control parameters to the values $d^* = 1.1314661145$ and $V_3^* = 1.038235081$, the first doublet of

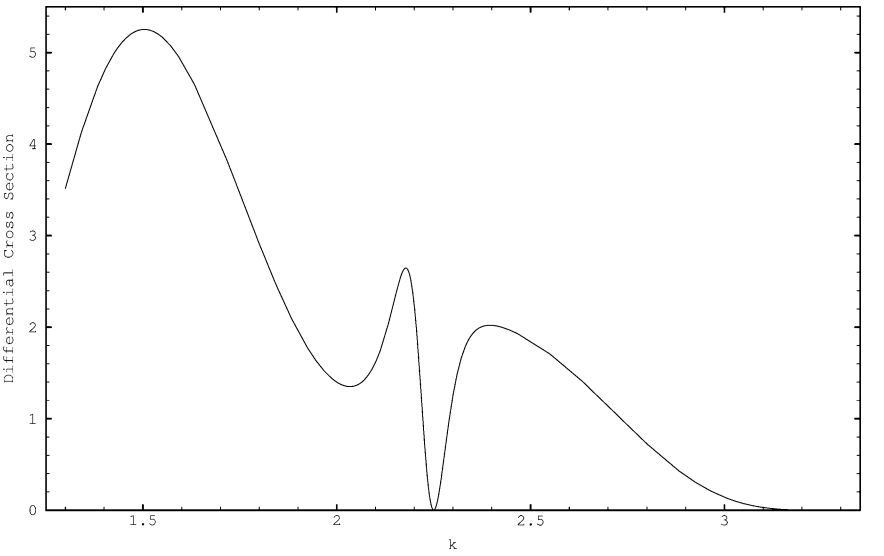

Fig. 2. Degeneracy of the doublet of resonances is brought about at $\tilde{k} = 2.22697606 - i0.07220139$ by fine tuning the parameters of the system as we described in the text. The split peak resonance is characteristic of a double pole in the scattering amplitude.

resonances becomes degenerate, with a precision better than one part in 10^8, at

$$\tilde{k} = 2.22697606 - i0.07220139. \tag{28}$$

At the resonance degeneracy, the cross section has a characteristic split peak. The splitting occurs because right at the middle of the degenerate resonance, the phase shift goes through π and the cross section vanishes, see Figs. 2 and 3.

Now let us turn our attention to the generalized Gamow eigenfunctions associated with a degeneracy of resonances. In the case of a one-channel problem with a short range, local potential and fixed angular momentum as the example we are considering here, the solution of the radial Schrödinger Eq. (1), which vanishes at the origin and behaves as a purely outgoing wave at distances larger than the range of the potential, is unique up to a multiplying constant. In other words, for each set of values of the external parameters (d, V_3) there is one and only one Gamow normalized eigenfunction $u_n(k_n, r)$ associated with each complex zero of the Jost function, k_n, lying in the fourth quadrant of the complex k-plane (Hernández *et al.*, 2003). When we move in parameter space from the point (d, V_3) where all complex energy eigenvalues (complex zeros of the Jost function) are different to a point (d^*, V_3^*) where two complex energy eigenvalues, say k_1^2 and k_2^2, are equal, the corresponding Gamow eigenfunction $u_1(k_1, r)$ and $u_2(k_2, r)$ go to a common

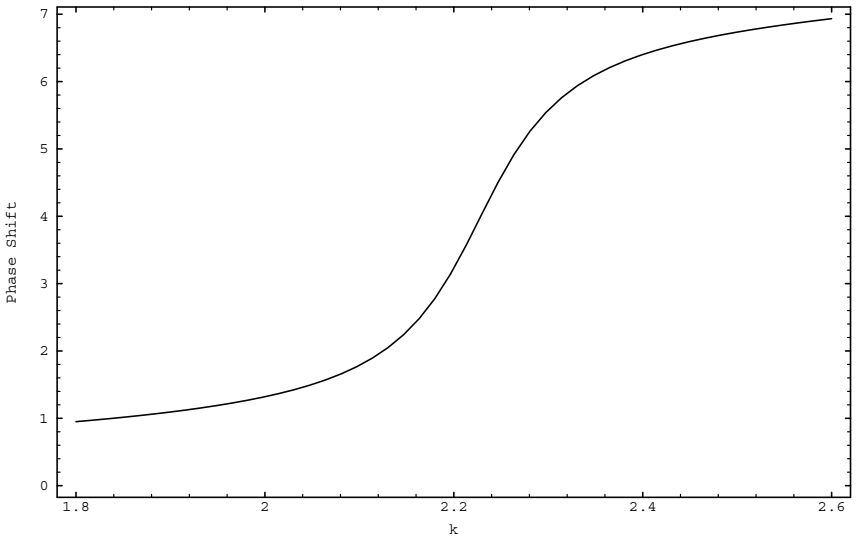

Fig. 3. The characteristic sharp increase by 2π of the phase shift, as a function of k, produced by a double resonance pole in the scattering amplitude. At the center of the double pole resonance, $k_0 = 2.2501818$, $\delta(k)$ goes through π.

limit $u_{\tilde{1}}(\tilde{k}, r)$. Hence, at degeneracy there is only one normal mode, the Gamow normalized eigenfunction $u_{\tilde{1}}(\tilde{k}, r)$ associated with the repeated (degenerate) energy eigenvalue $\tilde{k}^2$. However, another, linearly independent, generalized eigenfunction or abnormal mode is provided by the same limiting process that gives rise to the degeneracy. As we move in parameter space from the point (d, V_3) to the degeneracy point (d^*, V_3^*), the difference of the two eigenvalues that become degenerate vanish, and the difference of the corresponding Gamow eigenfunctions also vanish. Then, by continuity of $k_1(d, V_3)$ and $k_2(d, V_3)$ at the common limit $\tilde{k}(d^*, V_3^*)$, the derivative of the Gamow eigenfunction with respect to the complex energy eigenvalue exists:

$$\hat{u}_{\tilde{1}}(\tilde{k}, r) = \frac{2m}{\hbar^2}\frac{1}{2\tilde{k}} \lim_{|k_2-k_1|\to 0} \frac{u_2(k_2, r) - u_1(k_1, r)}{k_2 - k_1} = \frac{2m}{\hbar^2}\frac{1}{2\tilde{k}}\left(\frac{du_{\tilde{1}}(\tilde{k}, r)}{d\tilde{k}}\right). \quad (29)$$

The generalized Gamow eigenfunction, also called Gamow-Jordan eigenfunction (Hernández *et al.*, 2003) is

$$\hat{u}_{\tilde{1}}(\tilde{k}, r) = \frac{du_{\tilde{1}}(\tilde{k}, r)}{d\tilde{\mathcal{E}}} + c(\tilde{k})u_{\tilde{1}}(\tilde{k}, r), \quad (30)$$

where $\tilde{\mathcal{E}} = \hbar^2\tilde{k}^2/2m$, and $c(\tilde{k})$ is a function of $\tilde{k}$ but is independent of r,

$$c(\tilde{k}) = \frac{2m}{\hbar^2}\frac{1}{2\tilde{k}}\left[\frac{1}{\tilde{k}} - \frac{1}{2}\frac{1}{f(\tilde{k})}\frac{df(\tilde{k})}{d\tilde{k}} - \frac{1}{6}\left(\frac{d^2f(-k)}{dk^2}\right)_{\tilde{k}}^{-1}\left(\frac{d^3f(-k)}{dk^3}\right)_{\tilde{k}}\right]. \quad (31)$$

Therefore, when the Jost function has a double-resonance zero at $k = \tilde{k}$, there is a chain of Gamow-Jordan generalized eigenfunctions of length two, $\{u_{\tilde{1}}(\tilde{k}, r), \hat{u}_{\tilde{1}}(\tilde{k}, r)\}$, which are solutions of the Jordan chain of differential equations

$$-\frac{\hbar^2}{2m}\frac{d^2u_{\tilde{1}}(\tilde{k}, r)}{dr^2} + V(r)u_{\tilde{1}}(\tilde{k}, r) = \tilde{\mathcal{E}}u_{\tilde{1}}(\tilde{k}, r) \quad (32)$$

and

$$-\frac{\hbar^2}{2m}\frac{d^2\hat{u}_{\tilde{1}}(\tilde{k}, r)}{dr^2} + V(r)\hat{u}_{\tilde{1}}(\tilde{k}, r) = \tilde{\mathcal{E}}\hat{u}_{\tilde{1}}(\tilde{k}, r) + u_{\tilde{1}}(\tilde{k}, r), \quad (33)$$

and satisfy the same boundary conditions, namely, they vanish at the origin and at infinity they behave as outgoing waves.

In the particular case of a double barrier potential we are considering here

$$\hat{u}_{\tilde{1}}(\tilde{k}, r) = N_{\tilde{1}}^{-1}\left[\frac{m}{\hbar^2}\frac{1}{\tilde{k}}\left(\frac{\partial\phi(k, r)}{\partial k}\right)_{\tilde{k}} + c(\tilde{k})\phi(\tilde{k}, r)\right], \quad (34)$$

where $N_{\tilde{1}}$ is a normalization constant and $\phi(\tilde{k}, r)$ is given in Eqs. (2)–(13) and $\tilde{k}$ is given in (28).

The general theory of the Gamow-Jordan eigenfunctions associated with a degeneracy of unbound states is given by Hernández *et al.* (2003).

4. DEGENERACY OF UNBOUND STATES IN PARAMETER SPACE

The radial Hamiltonian H_r of a particle in a double barrier potential, introduced in (1) and (32) and (33), is a smooth function of the parameters of the potential barriers; five of these parameters were kept fixed, but the width of the inner barrier, d, and the depth of the second well, V_3, were allowed to vary. Therefore, we may consider the Hamiltonian H_r embedded in a population of Hamiltonians $H_r(d, V_3)$ smoothly parameterized by the two control parameters, d and V_3, which take values in some domain D of a manifold or parameter space. Each point in D represents a Hamiltonian H_r. In this section, we will be concerned with the topology of the surfaces representing the complex energy eigenvalues as function of (d, V_3) at a crossing of unbound states.

As explained in subsection 2.2, the energy eigenvalues of the radial Schrödinger equation are determined by the zeros of the Jost function, Eqs. (14) and (22).

Hence, when

$$
\begin{aligned}
f(-k_n) = \sin k_n r_1 &[\cosh(K_2(k_n)d) + \alpha_1(k_n)\sinh(K_2(k_n)d)] \\
&\times[\cos(K_3(k_n)(r_3 - r_2)) + \alpha_2(k_n, d)\sin(K_3(k_n)(r_3 - r_2))] \\
&\times \left\{ \frac{K_4(k_n, d)}{k_n}[\sinh(K_4(k_n, d)(r_4 - r_3)) \right. \\
&+ \alpha_3(k_n; d, V_3)\cosh(K_4(k_n, d)(r_4 - r_3))] - i[\cosh(K_4(k_n, d)(r_4 - r_3)) \\
&\left. + \alpha_3(k_n; d, V_3)\sinh(K_4(k_n, d)(r_4 - r_3))] \right\} \exp ik_n r_4 = 0. \qquad (35)
\end{aligned}
$$

is satisfied by k_n, with k_n lying in the fourth quadrant of the complex k-plane, the complex resonance energy eigenvalue is $\mathcal{E}_n = \hbar^2 k_n^2/2m$.

4.1. Energy Surfaces

The Jost function, $f(-k_n; d, V_3)$, occurring in (35) is a function of many variables. As a function of k, it is an analytic function of k-complex, but it is also explicitly dependent on the real valued control parameters (d, V_3). Therefore, the condition (35), implicitly defines the inverse functions

$$k_n(d, V_3) = f^{-1}(0; d, V_3), \quad n = 1, 2, \ldots \qquad (36)$$

as branches of a smooth, multivalued function of the parameters (d, V_3). Then, not only the radial Hamiltonian H_r, but also its complex energy eigenvalues $\mathcal{E}_n$ are smooth functions of the control parameters (d, V_3) in the domain D.

We solved numerically the implicit Eq. (36) for $k_1(d, V_3)$ and $k_2(d, V_3)$ in the neighborhood of, and at the crossing of unbound states. The results of the numerical computation of $k_1(d, V_3)$ and $k_2(d, V_3)$ were represented as a two-sheeted hypersurface in a Euclidean space with Cartesian coordinates $(\mathrm{Re}\, k, \mathrm{Im}\, k, d, V_3)$.

When the control parameters take the exceptional values $d^* = 1.1314661145$ and $V_3^* = 1.038235081$, the two resonance zeros of the Jost function, k_1 and k_2, coalesce in one double zero at $\tilde{k} = 2.22697606 - i0.0720139$, all other zeros remaining simple. At this point, the surfaces representing $k_1(d, V_3)$ and $k_2(d, V_3)$ touch each other and the corresponding complex energy eigenvalues, $\mathcal{E}_1$ and $\mathcal{E}_2$, become degenerate. In Fig. 4, the real function $\mathrm{Re}\, k_{1,2}(d, V_3)$ is shown as a surface S_R in the three-dimensional subspace with Cartesian coordinates $(\mathrm{Re}\, k, ., d, V_3)$. Similarly, in Fig. 5, the real function $\mathrm{Im}\, k_{1,2}(d, V_3)$ is shown as a surface, S_I in the three-dimensional subspace with Cartesian coordinates $(., \mathrm{Im}\, k, d, V_3)$.

From Figs. 4 and 5, it can be seen that, close to the exceptional point (d^*, V_3^*), where the two unbound states become degenerate, the function $\mathrm{Re}\, k_{1,2}(d, V_3)$ has

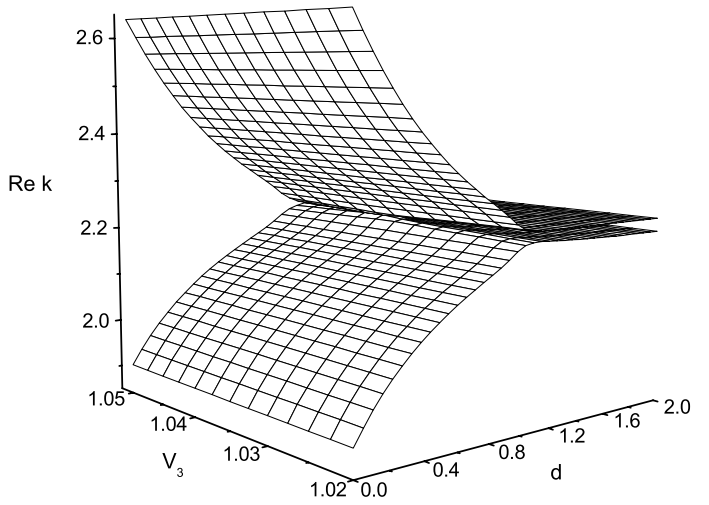

Fig. 4. The surface S_R that represents the real part of the eigenwave numbers k_1 and k_2 as functions of the control parameters (d, V_3) in the vicinity of a degeneracy of unbound states. This surface has two sheets which are copies of the plane (d, V_3) cut and joined smoothly along a line $\mathcal{L}_R$ that starts at the degeneracy or critical point (d^*, V^*) and runs to points such that $d > d^*$ and $V_3 > V_3^*$. Along $\mathcal{L}_R$, $\mathrm{Re}\, k_1 = \mathrm{Re}\, k_2$, but exact degeneracy of unbound states, $k_1 = k_2$, occurs only at the exceptional point with coordinates (d^*, V_3^*).

two branches and the surface S_R representing this function has two sheets which are glued together from two copies of the plane (d, V_3) which are cut and joined smoothly along a line $\mathcal{L}_R$. The projection of $\mathcal{L}_R$ on the plane (d, V_3) is a line $\mathcal{L}'$ see Fig. 6. The cut starts at the exceptional point on $\mathcal{L}_R$ with coordinates (d^*, V_3^*) and runs from this point to values of d larger than d^* and values of V_3 larger than V_3^*. The function $\mathrm{Im}\, k_{1,2}(d, V_3)$ also has two branches and the surface S_I representing this function is also glued from two copies of the plane (d, V_3) which are cut and joined smoothly along a line $\mathcal{L}_I$, as shown in Fig. 5. The projection of $\mathcal{L}_I$ on the plane (d, V_3) is also the line $\mathcal{L}'$ see Fig. 7. As in the case of $\mathrm{Re}\, k_{1,2}(d, V_3)$, the cut starts at the exceptional point on $\mathcal{L}_I$, but, in this case, the cut runs from the point (d^*, V_3^*) to values of d smaller than d^* and values of V_3 smaller than V_3^*.

The lines $\mathcal{L}_R$ and $\mathcal{L}_I$ are orthogonal to each other—they are in orthogonal subspaces—but have one point in common, the exceptional point with coordinates (d^*, V_3^*).

The projection of the lines $\mathcal{L}_R$ and $\mathcal{L}_I$ on the plane (d, V_3) are the two halves of the line $\mathcal{L}'$, as shown in Figs. 6 and 7. Close to the exceptional point the line $\mathcal{L}'$

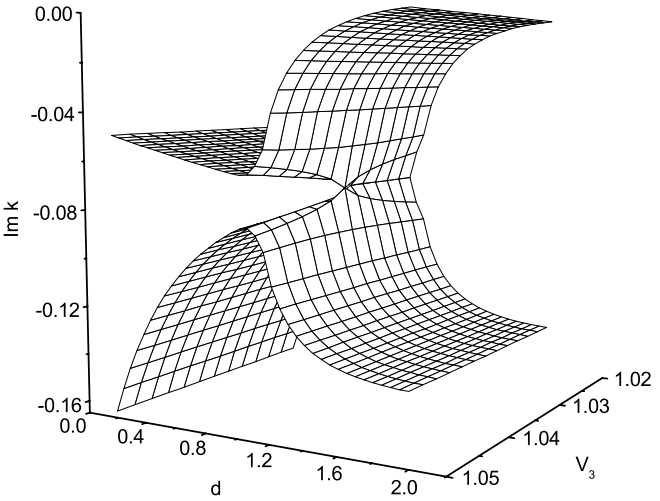

Fig. 5. The two-sheeted surface S_I that represents the imaginary part of eigenwave numbers k_1 and k_2 as functions of the control parameters (d, V_3) in the neighborhood of a degeneracy of unbound states with complex resonance energies $\mathcal{E}_1 = \hbar^2 k_i^2/2m$, $i = 1, 2$. This surface has two sheets which are copies of the plane (d, V_3) cut and joined smoothly along a line $\mathcal{L}_I$ that starts at the degeneracy (exceptional) point (d^*, V_3^*) and runs to points such that $d < d^*$ and $V_3 < V_3^*$. Along $\mathcal{L}_I$, Im $k_1 =$ Im k_2 but exact degeneracy, $k_1 = k_2$, occurs only at the exceptional point (d^*, V_3^*).

may be approximated by its tangent at the exceptional point

$$V_3 - V_3^* \approx m(d - d^*) \tag{37}$$

with $m \approx 0.19$.

Let us call Re $k_U(d, V_3)$ the function represented by points on the upper sheet of the surface S_R, and Re $k_L(d, V_3)$ the function represented by points on the lower sheet of the surface S_R. Likewise, let us call Im $k_U(d, V_3)$ the function represented by points on the upper sheet of the surface S_I and Im $k_L(d, V_3)$ the function represented by points on the lower sheet of the surface S_I.

Then, at the points on the line $\mathcal{L}_R$ such that $d' > d^*$ and $V_3' > V_3^*$,

$$\text{Re}\, k_U(d', V_3') = \text{Re}\, k_L(d', V_3'),$$

but

$$\text{Im}\, k_U(d' V_3') \neq \text{Im}\, k_L(d', V_3').$$

Similarly, at the points on the line $\mathcal{L}_I$, such that $d'' < d^*$ and $V_3'' < V_3^*$,

$$\text{Im}\, k_U(d'', V_3'') = \text{Im}\, k_L(d'', V_3'')$$

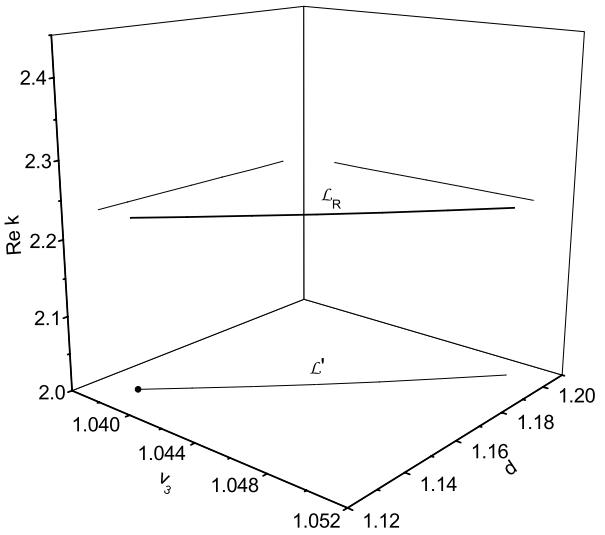

Fig. 6. The graph shows the cut $\mathcal{L}_R$ in the two-sheeted surface S_R that represents the two branched function $\mathrm{Re}\, k_{1,2}(d, V_3)$. The line $\mathcal{L}'$ is the projection of $\mathcal{L}_R$ in parameter space. The dot marks the exceptional point with coordinates (d^*, V_3^*).

but

$$\mathrm{Re}\, k_U(d'', V_3'') \neq \mathrm{Re}\, k_L(d'', V_3'')$$

At the exceptional point with coordinates (d^*, V_3^*), and only at that point, both, the real and imaginary parts of k_1 and k_2 are equal

$$k_1(d^*, V_3^*) = k_2(d^*, V_3^*).$$

Therefore, in the complex k-plane, the crossing point of the two simple zeros of the Jost function is an isolated point, where the Jost function has one double zero.

4.2. Sections of the Energy Hypersurface

Let us consider a point (d, V_3) in parameter space away from the exceptional point. That is, a point in the plane of the control parameters d and V_3 with Cartesian coordinates $(d, V_3) \neq (d^*, V_3^*)$. To this point corresponds a pair of non-degenerate eigenwave numbers

$$k_1(d, V_3) \neq k_2(d, V_3) \quad \text{if } (d, V_3) \neq (d^*, V_3^*),$$

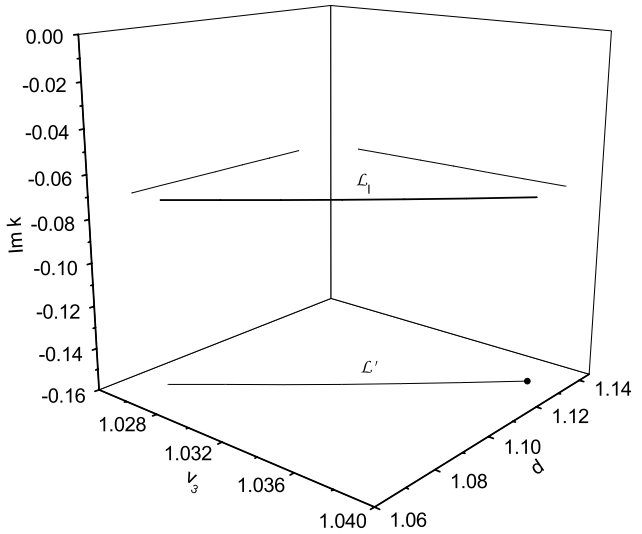

Fig. 7. The graph shows the cut $\mathcal{L}_I$ in the two-sheeted surface S_I that represents the two-branched function Im $k_{1,2}(d, V_3)$. The line $\mathcal{L}'$ is the projection of $\mathcal{L}_I$ on the plane (d, V_3). The dot marks the exceptional point with coordinates (d^*, V_3^*). Notice that the projections of $\mathcal{L}_R$ and $\mathcal{L}_I$ are the two halves of the same line $\mathcal{L}'$.

these two eigenwave numbers are represented by two points on the $k_{1,2}(d, V_3)$ hypersurface.

When the point (d, V_3) traces a path π in parameter space, the corresponding points $k_1(d, V_3)$ and $k_2(d, V_3)$ trace two curving trajectories, $C_1(\pi)$ and $C_2(\pi)$, on the $k_{1,2}(d, V_3)$ hypersurface. The topological structure of the hypersurface $k_{1,2}(d, V_3)$ will be most clearly evident in the shape and properties of the trajectories $C_1(\pi)$ and $C_2(\pi)$ for a path π that crosses the line $\mathcal{L}'$ at a point close to the exceptional point.

We define three straight line paths in parameter space, π_1, π_2 and π_3, by keeping the parameter V_3 fixed at some value $\bar{V}_3^{(i)}, i = 1, 2, 3$, and letting the parameter d vary. The values of $\bar{V}_3^{(i)}$ were chosen in such a way that the paths π_1, π_2 and π_3, cross the line $\mathcal{L}'$ at points located just before, at, and just after the exceptional point.

As a point moves in parameter space along the straight line path π_i from the starting point $(d_i, \bar{V}_3^{(i)})$ to the end point $(d_f, \bar{V}_3^{(i)})$, the points representing $k_1(d, V_3^{(i)})$ and $k_2(d, V_3^{(i)})$ move along the curving trajectories $C_1(\pi_i)$ and $C_2(\pi_i)$ on the hypersurface $k_{1,2}(d, V_3)$. The trajectories $C_1(\pi_i)$ and $C_2(\pi_i)$, are the intersection of the hypersurface $k_{1,2}(d, V_3)$ and the hyperplane $V_3 = \bar{V}_3^{(i)}$ in the space with Cartesian coordinates (Re k, Im k, d, V_3). Since V_3 is kept constant at the

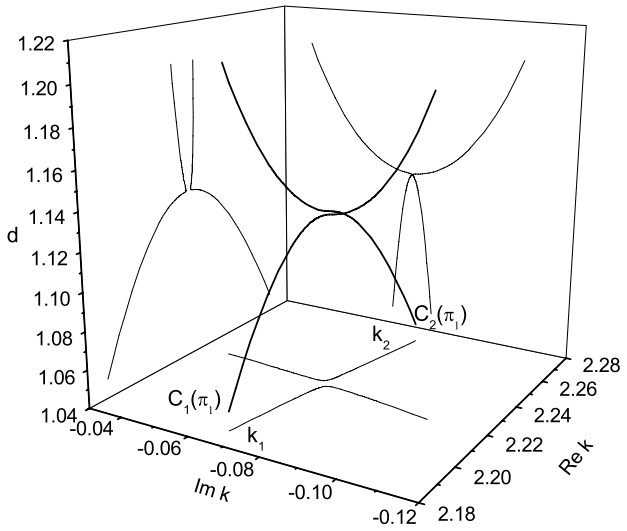

Fig. 8. The curves $C_1(\pi_1)$ and $C_2(\pi_1)$ are the trajectories traced by the points $k_1(d, \bar{V}_3^{(1)})$ and $k_2(d, \bar{V}_3^{(1)})$ on the hypersurface $k_{1,2}(d, \bar{V}_3^{(1)})$ when the point $(d, \bar{V}_3^{(1)})$ moves along the straight line path π_1 in parameter space. π_1 is defined by the conditions $1.05 \leq d \leq 1.20$, $V_3 = \bar{V}_3^{(1)} < V_3^*$; in the figure, π_1 runs parallel to the vertical axis and crosses the line $\mathcal{L}_I$ at a point $(\bar{d}^{(1)}, \bar{V}_3^{(1)})$ with $\bar{d}^{(1)} < d^*$, $\bar{V}_3^{(1)} < V_3^*$. The projections of $C_1(\pi_1)$ and $C_2(\pi_1)$ on the plane $(\mathrm{Im}\, k, d)$ are sections of the surface S_I; the projections of $C_1(\pi_1)$ and $C_2(\pi_1)$ on the plane $(\mathrm{Re}\, k, d)$ are sections of the surface S_R. The projections on the plane $(\mathrm{Re}\, k, \mathrm{Im}\, k)$ are the trajectories of the poles of the scattering matrix in the complex k-plane.

fixed value $\bar{V}_3^{(i)}$, the trajectories $C_1(\pi_i)$ and $C_2(\pi_i)$ may be represented as three dimensional curves in the space with Cartesian coordinates $(\mathrm{Re}\, k, \mathrm{Im}\, k, d)$.

The trajectories $C_1(\pi_i)$ and $C_2(\pi_i)$, for each path π_i were computed numerically. The results are shown as three-dimensional graphs in Figs. 8, 9 and 10. To each point on the trajectories $C_1(\pi_i)$ and $C_2(\pi_i)$ corresponds a triple of numbers $(\mathrm{Re}\, k_1, \mathrm{Im}\, k_1, d)$ and $(\mathrm{Re}\, k_2, \mathrm{Im}\, k_2, d)$ respectively, the numbers $(\mathrm{Re}\, k, \mathrm{Im}\, k, d)$ are shown in the figures as Cartesian coordinates. We show the trajectories $C_1(\pi_i)$ and $C_2(\pi_i)$ in perspective view and the three projections of these curves on the planes $(\mathrm{Re}\, k, d)$, $(\mathrm{Im}\, k, d)$ and on the complex k-plane $(\mathrm{Re}\, k, \mathrm{Im}\, k)$. Notice that, in each one of these figures, the path π_i is shown as the vertical axis Od, while in Figs. 4 and 5, Od is shown as a horizontal axis.

The properties of the trajectories $C_1(\pi_i)$ and $C_2(\pi_i)$ may now be readily understood in terms of the properties of the two sheeted surfaces S_R and S_I that represent the functions $\mathrm{Re}\, k_{1,2}(d, V_3)$ and $\mathrm{Im}\, k_{1,2}(d, V_3)$.

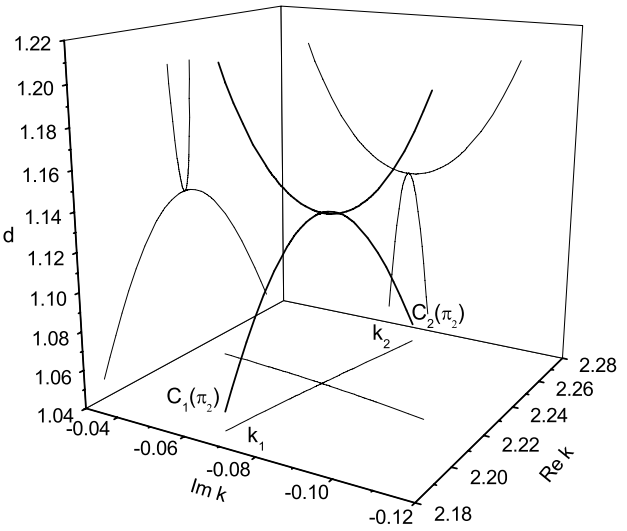

Fig. 9. $C_1(\pi_2)$ and $C_2(\pi_2)$ are the trajectories traced by the points $k_1(d, V_3)$ and $k_2(d, V_3)$ on the hypersurface $k_{1,2}(d, V_3)$ when the point (d, V_3) moves along the straight line path π_2 in parameter space. The path π_2 goes through the exceptional point (d^*, V_3^*); in the figure, π_2 runs parallel to the vertical axis and is defined by the condition $V_3 = V_3^*$. Notice the 90° turn made by $C_1(\pi_2)$ and $C_2(\pi_2)$ at the crossing (degeneracy) point. The three projections of $C_1(\pi_2)$ and $C_2(\pi_2)$ on the planes (Re k, d), (Im k, d) and (Re k, Im k) show a crossing.

Let us consider first Fig. 8, which shows the trajectories $C_1(\pi_1)$ and $C_2(\pi_1)$ traced by the points $k_1(d, V_3)$ and $k_2(d, V_3)$ on the hypersurface $k_{1,2}(d, V_3)$ when the point (d, V_3) moves along the straight line path π_1 in parameter space. The path π_1 is defined by the conditions

$$1.05 \leq d \leq 1.20 \quad \text{and} \quad \bar{V}_3^{(1)} = 1.0381,$$

it crosses the line $\mathcal{L}'$ to the left of the exceptional point at a point $\bar{d}^{(1)} = 1.1308$. Corresponding to this point, there is a point on the line $\mathcal{L}_I$ where the two sheets of S_I cross, but there is no corresponding point on the line $\mathcal{L}_R$ where the two sheets of S_R cross. Therefore, as the point d moves up on π_1, from the starting point at $d = 1.05$, the points Im $k_1(d, \bar{V}_3^{(1)})$ and Im $k_2(d, \bar{V}_3^{(1)})$ also move up and approaching each other on the upper and lower sheets of S_I respectively, until they meet when $d = \bar{d}^{(1)}$ and the two projections of $C_1(\pi_1)$ and $C_2(\pi_1)$ on the plane (Im k, d) cross at a point on the line $\mathcal{L}_I$ where the two sheets of S_I cross. After crossing, as d moves from $\bar{d}^{(1)} = 1.1308$ further up, the points Im $k_1(d, \bar{V}_3^{(1)})$ and Im $k_2(d, \bar{V}_3^{(1)})$ move now on the lower and upper sheets of S_I respectively

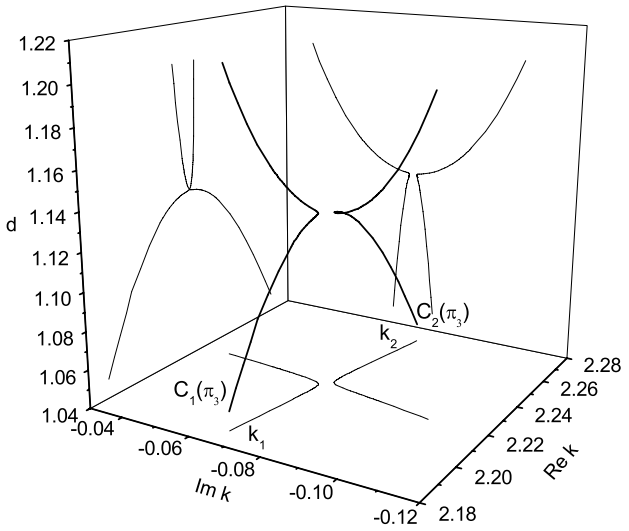

Fig. 10. The curves $C_1(\pi_3)$ and $C_2(\pi_3)$ are the trajectories traced by the points $k_1(d, V_3)$ and $k_2(d, V_3)$ on the hypersurface $k_{1,2}(d, V_3)$ when the point (d, V_3) moves along the straight line path π_3 in parameter space. π_3 is defined by the condition $V_3 = \bar{V}_3^{(3)}$ and, in the figure, runs parallel to the vertical axis; π_3 crosses the line $\mathcal{L}_R$ at a point $(\bar{d}^{(3)}, \bar{V}_3^{(3)})$ with $\bar{d}^{(3)} > d^*$ and $\bar{V}_3^{(3)} > V_3^*$. The projections of $C_1(\pi_3)$ and $C_2(\pi_3)$ on the plane $(\mathrm{Re}\, k, d)$ show a crossing, but the projections on the plane $(\mathrm{Im}\, k, d)$ and $(\mathrm{Re}\, k, \mathrm{Im}\, k)$ do not cross.

further up and away from each other, as shown in the projections on the plane $(\mathrm{Im}\ k, d)$ in Fig. 8. The points $\mathrm{Re}\, k_1(d, \bar{V}_3^{(1)})$ and $\mathrm{Re}\, k_2(d, \bar{V}_3^{(1)})$ can not cross, hence, as the point d moves up on π_1 from the starting point at $d = 1.05$, the points $\mathrm{Re}\, k_1(d, \bar{V}_3^{(1)})$ and $\mathrm{Re}\, k_2(d, \bar{V}_3^{(1)})$ also move up and approaching each other on the lower and upper sheets of S_R respectively, they come close together when $d = \bar{d}^{(1)}$, but since they cannot cross, when d moves further up, they also move further up and away from each other staying on the same lower and upper sheets of S_R they were at the initial value $d_i = 1.05$, as shown in the projections on the plane $(\mathrm{Re}\, k, d)$ in Fig. 8. We may now try to understand why is that, as d increases from the starting point at $d = 1.05$, the points $k_1(d, \bar{V}_3^{(1)})$ and $k_2(d, \bar{V}_3^{(1)})$ moving up on the trajectories $C_1(\pi_1)$ and $C_2(\pi_1)$ approach each other until they come close together when $d = \bar{d}^{(1)}$, but then, their trajectories make a sudden turn in opposite directions: $C_1(\pi_1)$ turns almost 90° towards smaller values of $\mathrm{Im}\ k$ and $C_2(\pi_1)$ turns almost 90° towards larger values of $\mathrm{Im}\ k$. As d moves further up on π_1, the points $k_1(d, \bar{V}_3^{(1)})$ and $k_2(d, \bar{V}_3^{(1)})$ move on $C_1(\pi_1)$ and $C_2(\pi_1)$ further up and away from each other. From Figs. 4 and 5, the sudden turn in the trajectories seem to be

produced by the crossing of Im $k_1(d, \bar{V}_3^{(1)})$ and Im $k_2(d, \bar{V}_3^{(1)})$ while Re $k_1(d, \bar{V}_3^{(1)})$ and Re $k_2(d, \bar{V}_3^{(1)})$ cannot cross, which means that Re $k_1 <$ Re k_2 for all values of $d \epsilon \pi_1$, while Im k_1 and Im k_2 can move freely from values Im $k_1 >$ Im k_2 to values Im $k_1 <$ Im k_2 when d moves along π_1 past the point $\bar{d}^{(1)}$.

Fig. 9 shows the trajectories $C_1(\pi_2)$ and $C_2(\pi_2)$ traced by the points $k_1(d, V_3)$ and $k_2(d, V_3)$ on the hypersurface $k_{1,2}(d, V_3)$ when the point (d, V_3^*) moves along the straight line path π_2 in parameter space. The path π_2 is defined by the conditions

$$1.05 \leq d \leq 1.20 \quad \text{and} \quad \bar{V}_3^{(2)} = V_3^* = 1.038235081$$

This path crosses the line $\mathcal{L}'$ precisely at the exceptional point. As explained above, at the exceptional point and only at that point, $k_1 = k_2$, the two lines $\mathcal{L}_I$ and $\mathcal{L}_R$ meet and the two sheets of each of the two surfaces S_R and S_I cross.

Therefore, as the point (d, V_3^*) moves on π_2 from the starting point at $d =$ 1.05 up to $d = d^*$, the points $k_1(d, V_3^*)$ and $k_2(d, V_3^*)$ move up on the trajectories $C_1(\pi_2)$ and $C_2(\pi_2)$, they approach each other until they meet when $d = d^*$. At this point, the trajectories make a sudden 90° turn in the same direction. This sudden 90° term is typical of a branch point singularity of square root type (rank one).

In a companion paper (Hernández *et al.*, 2007), we argued that, when discussing the mixing properties of an isolated doublet of unbound states, it is convenient to write the $S-$matrix poles, k_1, and k_2, in terms of a pole position function $k_{1,2}$ as

$$k_1(d, V_3) = K(d, V_3) + k_{1,2}(d, V_3) \tag{38}$$

and

$$k_2(d, V_3) = K(d, V_3) - k_{1,2}(d, V_3) \tag{39}$$

where

$$K = \frac{1}{2}(k_1(d, V_3) + k_2(d, V_3)) \tag{40}$$

and

$$k_{1,2} = \sqrt{\frac{1}{4}(k_1(d, V_3) - k_2(d, V_3))^2} \tag{41}$$

In Hernández *et al.* (2007), it was shown that the functions $K(d, V_3)$ and $k_{1,2}^2(d, V_3)$ are regular functions of the parameter (d, V_3) at the exceptional point (d^*, V_3^*) and may be expanded in a Taylor series about this point. Hence

$$k_{1,2} \approx [\mathfrak{c}_1(d - d^*) + \mathfrak{c}_2(V_3 - V_3^*)]^{1/2}, \tag{42}$$

For values of the parameters (d, V_3) on the path π_2 just before the crossing, $V_3 = V_3^*$ and $d = d^* - \eta$ with $\eta > 0$.

$$k_{1,2}(\pi_2) \approx \exp(i\pi/2)[\mathfrak{c}_1\eta]^{1/2}. \tag{43}$$

For values of (d, V_3) in the path π_2, just after the crossing, with, $V_3 = V^*$ and $d = d^* + \eta$, and $\eta > 0$,

$$k_{1,2}(\pi_2) \approx [\mathfrak{c}_1 \eta]^{1/2}. \tag{44}$$

Therefore, just before the crossing, we have

$$k_1(d^* - \eta, V_3^*) \approx K(d^*, V_3^*) + \exp(i\pi/2)[\mathfrak{c}_1 \eta]^{1/2}, \tag{45}$$

$$k_2(d^* - \eta, V_3^*) \approx K(d^*, V_3^*) - \exp(i\pi/2)[\mathfrak{c}_1 \eta]^{1/2}, \tag{46}$$

and, just after the crossing, we get

$$k_1(d^* + \eta, V_3^*) \approx K(k^*, V_3^*) + [\mathfrak{c}_1 \eta]^{1/2} \tag{47}$$

and

$$k_2(d^* + \eta, V_3^*) \approx K(k^*, V_3^*) - [\mathfrak{c}_1 \eta]^{1/2}. \tag{48}$$

The sudden 90° turn at the exceptional point observed in the numerical computation of the trajectories, traced by the points k_1 and k_2 on the $k_{1,2}$ hypersurface is a clear indication that this function has a branch point singularity of square root type at the exceptional point.

Finally, Fig. 10 shows the trajectories $C_1(\pi_3)$ and $C_2(\pi_3)$ traced by the points $k_1(d, V_3)$ and $k_2(d, V_3)$ on the hypersurface $k_{1,2}(d, V_3)$ when the point (d, V_3) moves along the straight line path π_3 in parameter space. The path π_3 is defined by the condition

$$1.05 \leq d \leq 1.20 \quad \text{and} \quad \bar{V}_3^{(3)} = 1.0384 \tag{49}$$

this path crosses the line $\mathcal{L}'$ to the right of the exceptional point at the point $\bar{d}^{(3)} = 1.132$. Corresponding to the point $\bar{d}^{(3)}$, there is a point on the line $\mathcal{L}_R$ where the two sheets of S_R cross, but there is no corresponding point on the line $\mathcal{L}_I$ where the two sheets of the surface S_I cross. Hence, as the point $(d, \bar{V}_3^{(3)})$ moves up on π_3, the points $\mathrm{Re}\, k_1(d, \bar{V}_3^{(3)})$ and $\mathrm{Re}\, k_2(d, \bar{V}_3^{(3)})$ also move up and approach each other on the lower and upper sheets of S_R respectively, until they meet when $d = \bar{d}^{(3)}$ and the two projections of $C_1(\pi_3)$ and $C_2(\pi_3)$ on the plane $(\mathrm{Re}\, k, d)$ cross. After crossing, as d moves further up, the points $\mathrm{Re}\, k_1(d, \bar{V}_3^{(3)})$ and $\mathrm{Re}\, k_2(d, \bar{V}_3^{(3)})$ move up and away from each other on the upper and lower sheets of S_R respectively as shown in the projections on the plane $(\mathrm{Re}\, k, d)$ in Fig. 10. The points $\mathrm{Im}\, k_1(d, \bar{V}_3^{(3)})$ and $\mathrm{Im}\, k_2(d, \bar{V}_3^{(3)})$ cannot cross, therefore, as the point d moves up on π_3 from the starting point at $d_i = 1.05$, the points $\mathrm{Im}\, k_1(d, \bar{V}_3^{(3)})$ and $\mathrm{Im}\, k_2(d, \bar{V}_3^{(3)})$ also move up and approach each other on the upper and lower sheets of S_I respectively, they come close together when $d = \bar{d}^{(3)}$, but since they cannot cross, when d moves further up they also move further up and away from each other staying on the same upper and lower sheets of S_I where they were at the initial value $d_i = 1.05$, as shown in the projections on the plane $(\mathrm{Im}\, k, d)$ in Fig. 10.

The sudden turn in the trajectories is produced by two effects, one is the crossing of $\mathrm{Re}\, k_1(d, \bar{V}_3^{(3)})$ and $\mathrm{Re}\, k_2(d, \bar{V}_3^{(3)})$ while $\mathrm{Im}\, k_1(d, \bar{V}_3^{(3)})$ and $\mathrm{Im}\, k_2(d, \bar{V}_3^{(3)})$ cannot cross which means that $\mathrm{Im}\, k_1(d, \bar{V}_3^{(3)}) > \mathrm{Im}\, k_2(d, \bar{V}_3^{(3)})$ for all values of d on π_3, while $\mathrm{Re}\, k_1$ and $\mathrm{Re}\, k_2$ can move freely from values $\mathrm{Re}\, k_1 < \mathrm{Re}\, k_2$ to values $\mathrm{Re}\, k_1 > \mathrm{Re}\, k_2$ when d moves along π_3 past the point $\bar{d}^{(3)}$. The other effect is the change in phase of $k_{1,2}$ due to the change in sign of the term $\mathfrak{c}_1(d - \bar{d}^{(3)})$ under the square root in the right hand side of the equation

$$k_{1,2}(\pi_3) \approx \left[\mathfrak{c}_1(d - \bar{d}^*) + \mathfrak{c}_2\left(\bar{V}_3^{(3)} - V_3^*\right)\right]^{1/2}. \tag{50}$$

Making use the equation (37) for points on the line $\mathcal{L}'$, $k_{1,2}(\pi_3)$ may be written as

$$k_{1,2}(\pi_3) \approx \left[\mathfrak{c}_1\left(d - \bar{d}^{(3)}\right) + (\mathfrak{c}_1 + m\mathfrak{c}_2)\left(d^{(3)} - d^*\right)\right]^{1/2}, \tag{51}$$

since $\mathfrak{c}_1$ and $\mathfrak{c}_2$ are complex $k_{1,2}(\pi_3)$ never vanishes, but when the term $\mathfrak{c}_1(d - \bar{d}^{(3)})$ changes sign, $k_{1,2}(\pi_3)$ makes a sudden turn.

5. CONCLUSIONS

In this paper we discussed some aspects of the degeneracy of unbound states in the scattering of a beam of particles by a double barrier potential. It was shown that degeneracies of unbound states (resonances) and the concomitant double poles of the scattering matrix may easily be brought about by adjusting the values of only two real independent parameters in the Hamiltonian of the system, so as to satisfy the degeneracy conditions. In the example discussed here, the control parameters of the system are the width, d, of the inner barrier and the depth, V_3, of the external potential.

The resonance energy eigenvalues $\mathcal{E}_n = \hbar k_n^2/2m$, and the corresponding complex eigenwave numbers k_n are smooth functions of the control parameters. In the vicinity of a degeneracy of two unbound states with complex energy eigenvalues $\mathcal{E}_1$ and $\mathcal{E}_2$, the resonance conditions define the corresponding wave numbers, $k_1(d, V_3)$ and $k_2(d, V_3)$, as branches of a multivalued function $k_{1,2}(d, V_3)$.

With the purpose of exploring the geometrical and topological properties of the hypersurface representing $k_{1,2}(d, V_3)$ in parameter space, we solved numerically the implicit equation for $k_1(d, V_3)$ and $k_2(d, V_3)$ in the neighborhood of, and at a degeneracy of unbound states.

We found that, close to the degeneracy of unbound states,

1. The function $\mathrm{Re}\, k_{1,2}(d, V_3)$ has two branches and is represented by a two sheeted surface S_R. The two sheets of S_R are two copies of the plane (d, V_3) which are cut and joined smoothly along a line $\mathcal{L}_R$ starting at the exceptional point and extending to values $d \geq d^*$ and $V_3 \geq V_3^*$.

2. The function Im $k_{1,2}(d, V_3)$ also has two branches and is represented by a two sheeted surface S_I. The two sheets of S_I are two copies of the plane (d, V_3) which are cut and pasted smoothly along a line $\mathcal{L}_I$ extending from the exceptional point to values $d \leq d^*$ and $V_3 \leq V_3^*$.
3. The projections of the lines $\mathcal{L}_R$ and $\mathcal{L}_I$ on the plane (d, V_3) are the two halves of a line $\mathcal{L}'$ that goes through the exceptional point (d^*, V_3^*).
4. At the exceptional point, and only at that point, both the real and imaginary parts of k_1 and k_2 are equal. Therefore, in the complex k-plane, at the crossing point, the two simple zeros of the Jost function merge into one double zero which is an isolated point (no branch cuts in the k-plane).

We also computed sections, $V_3 = \bar{V}_3$, of the hypersurface representing $k_{1,2}(d, V_3)$. These sections were represented as trajectories $C_1(\pi)$ and $C_2(\pi)$ traced by the points $k_1(d, \bar{V}_3)$ and $k_2(d, \bar{V}_3)$ on the hypersurface $k_{1,2}(d, V_3)$ when the point (d, V_3) traces a straight line path π in parameter space; π is defined by the conditions $V_3 = \bar{V}_3$ and $1.05 \leq d \leq 1.2$ for various values of $\bar{V}_3$.

A careful examination of the properties of the surfaces S_R and S_I and the trajectories $C_1(\pi_i)$ and $C_2(\pi_i)$ for various paths π_i suggests that the topological structure of the hypersurface representing $k_{1,2}(d, V_3)$ is the same as the topological structure of the surface of the square root function in the right hand side of the expression

$$k_{1,2}(d, V_3) \approx K(d, V_3) \pm \sqrt{\mathfrak{c}_1(d - d^*) + \mathfrak{c}_2(V_3 - V_3^*)}, \tag{52}$$

where $\mathfrak{c}_1$ and $\mathfrak{c}_2$ are complex constants.

In our previous papers on the degeneracy and crossing of resonances (Mondragón and Hernández, 1993, 1996), see also (Hernández *et al.*, 2003) we had found essentially the same result written in a slightly different form, namely

$$k_{1,2}(d, V_3) = K(d, V_3) \pm \sqrt{\left(\vec{R} - i\frac{1}{2}\vec{\Gamma}\right)^2}, \tag{53}$$

where $\vec{R}(d, V_3)$ and $\vec{\Gamma}(d, V_3)$ are real vectors with Cartesian components $(x, 0, z)$ and $(\Gamma_x, 0, \Gamma_z)$. The components x, z, Γ_x and Γ_z are regular functions of the control parameters in a neighborhood of the critical point. Expanding $\vec{R}$ and $\vec{\Gamma}$ in Taylor series about the critical point, and keeping only terms of the first order in $(d - d^*)$ and $(V_3 - V_3^*)$, Eq. (53) takes the form

$$k_{1,2}(d, V_3) \approx K(d, V_3) \pm \sqrt{\left(\vec{R}_0 - i\frac{1}{2}\vec{\Gamma}_0\right)^2 + \mathfrak{c}_1(d - d^*) + \mathfrak{c}_2(V_3 - V_3^*)}, \tag{54}$$

which is essentially the same as in (52).

The degeneracy conditions, are

$$R_0^2 - \frac{1}{4}\Gamma_0^2 = 0 \quad \text{and} \quad \vec{R}_0 \cdot \vec{\Gamma}_0 = 0,$$

as in our previous papers (Mondragón and Hernández, 1993, 1996; Hernández *et al*., 2003).

In conclusion, some geometric and topological properties of a degeneracy of unbound or resonant states were explicitly exhibited in a simple model of the scattering of a beam of particles by a double barrier potential with two regions of trapping. We found that, in the vicinity of a degeneracy of unbound states, the surfaces that represent the complex resonance eigenwave numbers as functions of two real control parameters have the same topology as the surface of a square root of the difference of two complex regular functions of the real control parameters. The characteristic behavior of crossings and anticrossings of the energies and widths of an isolated doublet of unbound states, observed in the vicinity of a degeneracy when one control parameter of the system is moved, is explained in terms of the topology of the surface that represents the complex energy resonance eigenvalues in parameter space.

ACKNOWLEDGMENTS

We thank Professor Peter von Brentano (Universität zu Köln) for many inspiring discussions on this exciting problem.

This work was partially supported by CONACyT México under Contract No. 40162-F and by DGAPA-UNAM Contract No. PAPIIT: IN116202.

REFERENCES

Alden Mead, G. (1992). *Reviews of Modern Physics* **64**, 51.

Berry, M. V. (1984). *Proceedings of the Royal Society London Series A* **392**, 45.

Berry, M. V. (1985). Aspects of Degeneracy. In *Chaotic Behaviour in Quantum Systems*, G. Casati, (ed.), NATO ASI Series **B 120** Plenum, New York, p. 123.

Dembowski C., Dietz, B., Gräf, H. L., Herney, H. L., Heine, A., Heiss, W. D., and Richter, A. (2003). *Physical Review Letters*. **90**, 034101-1.

Dembowski C., Gräf H. L., Harney, H. L., Heine, A., Heiss, W. D., Rehfeld, H., and Richter, A. (2001). *Physical Review Letters*. **86**, 787.

For collections of basic papers on geometric phases see the monographs *Geometric Phases in Physics* F. Wilczek, and A. A., Shapere, (eds.) World Scientific, Singapore (1989); *Topological Phases in Quantum Theory* B., Markovsky, and V.I., Vinitsky, (eds). World Scientific (1989), Singapore.

For reviews on Berry's phase see: Jackiw, R. (1988). *Communications in Molecular Physics* **21**, 71.

Friedrich, H. and Wintgen, D. (1985). *Physical Review A* **32**, 3231.

Heiss, W. D. (1999). *European Physical Journal D* **7**, 1.

Hernández, E., Jáuregui, A., and Mondragón, A. (1992). *Revista Mexicana de Fisica* **38**(S2), 128.

Hernández, E., Jáuregui, A., and Mondragón, A. (2000). *Journal of Physics A: Mathematical and General* **33**, 4507.

Hernández, E., Jáuregui, A., and Mondragón, A. (2003). *Physical Review A* **67**, 022721-1.
Hernández, E., Jáuregui, A., Mondragón, A., and Nellen L. (2007). *International Journal of Theoretical Physics*, this same issue.
Hernández, E. and Mondragón, A. (1994). *Physics Letters B* **326**, 1.
Keck, F., Korsch H. J., and Mossmann, S. (2003). *Journal of Physics A: Mathematical and General* **36**, 2125.
Korsch H. J. and Mossmann, S. (2003). *Journal of Physics A: Mathematical and General* **36**, 2139.
Mondragón, A. and Hernández, E. (1993). *Journal of Physics A: Mathematical and General* **26**, 5595.
Mondragón, A. and Hernández, E. (1996). *Journal of Physics A: Mathematical and General* **29**, 2567.
Mondragón, A. and Hernández, E. (1998). Accidental degeneracy and Berry phase of resonant states, in *Irreversibility and Causality: Semigroups and Rigged Hilbert Sapce* A., Bohm, H.-D., Doebner, and P., Kielanowski (eds). (Lecture Notes in Physics), vol. **504**, Springer-Verlag, Berlin, p. 257.
Moore, D. J. (1990). *Physics Reports* **210**, 1.
Philipp, M., von Brentano, P., Pascovici, G., and Richter, A. (2000). *Physical Review E* **62**, 1922.
Teller, E. (1937). *Journal of Physical Chemistry* **41**, 109.
Vanroose, W. (2001). *Physical Review A* **64**, 062708-1.
Vanroose, W., Leuven, P., Arickx, F., and Broeckhove, J. (1997). *Journal of Physics A: Mathematical and General* **30**, 5543.
Vinitski, S. J., *et al*., (1990). *Soviet Physics-Uspekhi* **33**, 40 3.
von Brentano, P. (1990). *Physics Letters B* **238**, 1.
von Brentano, P. (1996). *Physics Reports* **264**, 57.
von Brentano, P. and Philipp, M. (1999). *Physics Letters B* **454**, 171.
von Neumann, J. and Wigner, E. P. (1929). *Physikalische Zeitshrift* **30**, 467.
Zwanziger, J. W., Rucker, S. P., and Chingas, G. C. (1991). *Physical Reveiw A* **43**, 3232.